THE ASTROPHYSICAL JOURNAL, 384:656–664, 1992 January 10
© 1992. The American Astronomical Society. All rights reserved. Printed in U.S.A.

MULTIFREQUENCY OBSERVATIONS OF A REMARKABLE SOLAR RADIO BURST

S. M. WHITE AND M. R. KUNDU
Astronomy Program, University of Maryland, College Park, MD 20742
T. S. BASTIAN
National Radio Astronomy Observatory, P.O. Box 0, Socorro, NM 87801
D. E. GARY AND G. J. HURFORD
Caltech, Solar Astronomy 264-33, Pasadena, CA 91103
T. KUCERA
University of Colorado, APAS, Boulder, CO 80309-0391
AND
J. H. BIEGING
Radio Astronomy Laboratory, University of California at Berkeley, and Steward Observatory, University of Arizona, Tucson, AZ 85721
Received 1991 May 2; accepted 1991 July 17

ABSTRACT

Observations of an impulsive solar radio burst from three observatories are presented. The striking observational aspects of this flare are that the time profile was identical throughout at 8.6, 15, and 86 GHz, that the spectrum was apparently flat from 15 to 86 GHz, and that there was a sharp cutoff in the spectrum between 5.0 and 8.6 GHz. The simplest interpretation of the cutoff, namely as a plasma frequency effect, leads to the conclusion that there was exceptionally high-density material in the solar corona ($\sim 5 \times 10^{11}$ cm^{-3}). Very Large Array images at 15 GHz show a single loop structure which brightened uniformly and showed little change in size during the whole impulsive phase. The flat spectrum is consistent with optically thin thermal bremsstrahlung emission, but the lack of observed soft X-ray emission and other properties of the flare cannot easily be accommodated by this mechanism. We also explore the possibility that the emission is optically thick due to thermal absorption of nonthermal gyrosynchrotron emission, or optically thin gyrosynchrotron emission absorbed by high-density material intervening along the line of sight. Both of these explanations also face difficulties.

Subject headings: Sun: flares — Sun: radio radiation — radiation mechanisms: cyclotron and synchrotron

1. INTRODUCTION

During 1989 June an international campaign of solar observations was conducted to study solar flares. On June 23 the Berkeley-Illinois-Maryland millimeter-wavelength array (BIMA), the Caltech frequency-agile interferometer at Owens Valley Radio Observatory (OVRO), and the Very Large Array (VLA)[1] all detected a weak impulsive burst at 22:25 UT. Here we report on these observations and their implications. Most impulsive solar radio bursts show radio spectra consistent with gyrosynchrotron emission from inhomogeneous sources with magnetic field strengths of several hundred G. Such spectra typically have a peak near 10 GHz and a high-frequency spectral index of -3 to -5 (Guidice & Castelli 1975). This burst has quite a different spectrum. The excellent coverage of this burst across a broad range of frequencies, at high temporal and spatial resolution, should offer an excellent opportunity to model the burst source. However, we are presently unable to find a self-consistent model which can explain all the observed properties of this burst.

[1] The Very Large Array is a facility of the National Radio Astronomy Observatory, which is operated by Associated Universities, Inc., under cooperative agreement with the National Science Foundation.

2. OBSERVATIONS AND ANALYSIS

2.1. *Berkeley-Illinois-Maryland Array (BIMA)*

The BIMA array presently consists of three 6 m dishes operating in the 3 mm wavelength atmospheric window. For observations of solar flares it is used as a simple interferometer in one linear polarization (equivalent to Stokes *I*) with one or three baselines giving fringe spacings on the sky of 1″–15″, depending on the array configuration (Kundu et al. 1990). For these observations we used observing software modified by R. Plambeck to allow ~0.39 s time resolution (with an integration time of 0.32 s).

A number of bursts were detected during the campaign period. Here we report only on a burst on 1989 June 23 at 22:25 UT. At this time the only baseline available was an east–west baseline of 97 m, providing an interferometer fringe spacing of 9″. Such an interferometer can measure only the total flux of sources smaller than about 3″. The active region AR 5555 was at the center of the 2′ field of view.

The time profile of the burst at 86 GHz is shown in Figure 1. It consists of a simpler linear rise in 5.7 s, followed by a smooth decay. The decay can be followed for about 90 s and can be well fitted by two exponential decays: for the first 15 s the decay has an *e*-folding time of 18 s, and thereafter it has an *e*-folding time of 32 s.

Amplitude calibration was carried out using the solar observing software on standard calibration sources. Unfor-

© American Astronomical Society • Provided by the NASA Astrophysics Data System

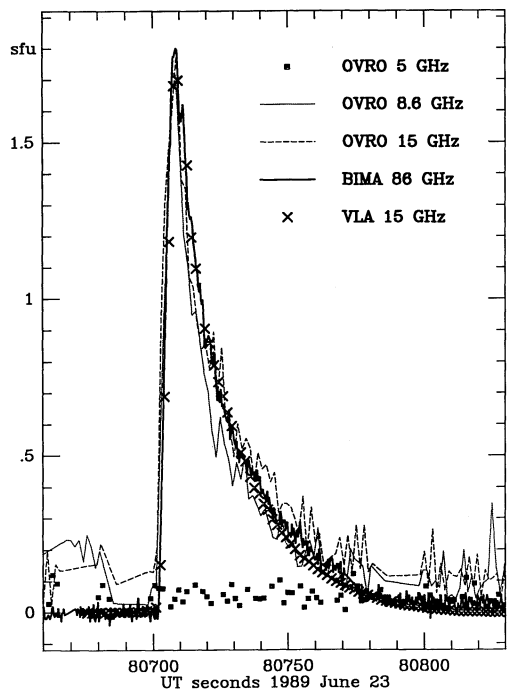

FIG. 1.—The time profiles of the radio emission observed by BIMA at 86 GHz (*solid line*), by OVRO at 5.0 (*filled squares*), 8.6 (*dotted line*), and 15.0 GHz (*broken line*); and by the VLA at 15 GHz (*crosses*). The time axis is in UT s (note that 80,700 s corresponds to 22:25:00 UT). The 8.6 and 15 GHz profiles have been normalized to match the 86 GHz peak flux of 1.8 sfu in order to facilitate comparison.

tunately we do not have an absolute calibration accurate to better than 30% for this period. We estimate the peak flux of the burst at BIMA to be 1.8 ± 0.6 sfu. The preflare level was about 0.05 sfu, and the rms noise level was about 0.01 sfu.

2.2. *Owens Valley Radio Observatory Frequency-Agile Interferometer*

The OVRO frequency-agile interferometer (Hurford, Read, & Zirin 1984) consists of a three-element interferometer observing at 45 frequencies between 1 and 18 GHz. On this day a nonstandard observing mode was being followed in order to match the observations at the VLA. Five integrations in one linear polarization, of 100 millisecond each, were made consecutively at 5.0, 8.6, and 15.0 GHz, giving a time resolution of 1.5 s. In addition, every 100 s a standard 45 frequency spectrum was taken over 10 s; however, such a spectrum was taken immediately prior to the onset of the burst and consequently no spectra were taken during the burst.

The time profiles of the emission observed by OVRO at 8.6 and 15 GHz appear to match the time profile at 86 GHz well, although there is a suggestion that the 8.6 GHz curve decays slightly faster than the higher frequencies. A peak flux of 2.7 ± 0.3 sfu at 8.6 GHz was obtained; unfortunately, no good calibration at 15 GHz was available, but an estimate from the total power data which assumes that the mean active region brightness temperature is at $20\text{–}30 \times 10^3$ K (see below) gives a flux consistent with the VLA 15 GHz flux of 1.85 sfu. There was no burst emission detected at 5.0 GHz: the flux level during the burst averaged 0.06 sfu with an rms of 0.03 sfu. Note that 5.0 GHz is the most sensitive and well-calibrated of the three frequencies observed by OVRO on this day, and no technical problems were detected. Plots of amplitude and phase at 5 GHz before, during, and after the burst show the usual characteristics of the response of OVRO to activate region emission. Other bursts were seen at 5.0 GHz on the same day.

At this time the three antennas were all along an east–west track, giving fringe spacings of 24″, 15″, and 9″ at 8.6 GHz on the three baselines, respectively. All three baselines measured the same flux at 8.6 GHz, and, assuming a Gaussian cross section and a measurement uncertainty of 10%, the source dimension can be determined to be no bigger than 2″ east–west. This is in agreement with the 15 GHz VLA images to be discussed next.

2.3. *Very Large Array*

The VLA was used in the C-configuration to carry out joint observations in two subarrays. One subarray was dedicated to continuous monitoring at 15 GHz; the other time-shared between 5 and 8.6 GHz. An integration time of 1.66 s was used. For the duration of the radio burst near 22:25 UT the VLA was observing at 5 and 15 GHz. Unfortunately, problems with the correlator corrupted the 5 GHz data, rendering it unusable. The 15 GHz data were only slightly affected, with only two data records lost during the course of the burst.

A map of the preburst active region at 15 GHz showed the presence of a small (7″), amorphous source with a peak brightness of 3.6×10^4 K and a mean brightness of 3.0×10^4. Its maximum was displaced by 2″ from the subsequent burst. The preburst visibilities were vector-subtracted from the 15 GHz data base and the remainder self-calibrated in phase to remove residual errors in the antenna-based phase. Maps were made of the burst for each 1.66 s integration and in each sense of circular polarization for the duration of the burst. The variation of the total intensity as a function of time was obtained by integrating over the source for each snapshot image (Fig. 1). The degree of circular polarization assumes a relatively constant value of $\sim 25\%$ throughout. Figure 2 shows a snapshot map of the total intensity brightness temperature distribution at the peak of the burst (snapshot maps at other times and in circularly polarized flux are essentially identical).

The burst source may be characterized as a single, looplike structure which changes little in aspect over time. Its dimensions are roughly 5×10^8 cm in length and 1.5×10^8 cm in width. The images show no obvious evolution of source size except for a slight contraction during the decay. Because the source size changes little in time, the source brightness temperature tracks the total flux. The peak brightness temperature at 15 GHz is 1.1×10^7 K.

2.4. *Relative Timing*

We have carefully compared the BIMA data (0.39 s time resolution) with the OVRO 8.6 and 15 GHz time profiles (1.5 s resolution) and the VLA 15 GHz time profile (1.7 s resolution) by rescaling them so that they all have the same peak flux. To within the limits imposed by the noise levels, which are somewhat higher in the OVRO data than in the BIMA and VLA data, we can find no significant differences between the profiles at the three frequencies, except for a period during the decay phase (80720–80730) when the 8.6 GHz curve appears to drop slightly faster than the other frequencies.

© American Astronomical Society • Provided by the NASA Astrophysics Data System

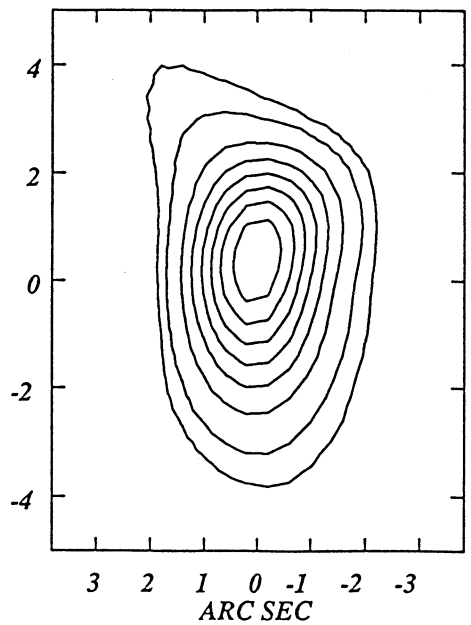

FIG. 2.—A contour plot of the brightness temperature of the radio burst at its peak made from VLA data at 15 GHz. The beam size was 1.″9 × 1.″3. The burst source showed effectively no evolution in time. Contours are at 1, 2, 3, 4, 6, 8, 10, 12, and 14 × 7 × 10^5 K. The rms noise level in the map is at about 1.5 × 10^5 K. The direction of celestial north is toward the top of these images.

2.5. *Other Observations*

This was a small burst by usual standards, and although many observatories were tracking AR 5555 on this day we can find no reports of detection of this burst at other wavelengths. There is no peak in the *GOES* profile at the time of the burst, and the background level of the 1–8 Å flux was just above C1. Initially, no obvious burst was seen in the region on the Big Bear Solar Observatory high-resolution Hα images, but after careful comparison of the Hα and VLA source locations, we have found the Hα counterpart. It is an extremely small brightening far below subflare level as seen in centerline Hα, and not visible at all in Hα–0.6 Å off-band. Figure 3 shows four panels which indicate the optical location of the event. Figure 3*a* shows the region ~1 minute before the event, while Figure 3*b* shows the same region during the event (at 22:25:38 UT or 80738.0 s UT). The dimension of the Hα brightening is comparable with the size of the VLA source (5″–10″). To help locate the event relative to other features, Figure 3*c* shows a longitudinal magnetogram, and Figure 3*d* shows an off-band Hα image. The small brightening seen in Figure 3*b* is located in a small spot group, as shown in Figure 3*d*, of positive magnetic polarity (Fig. 3*c*), but with a negative polarity spot nearby. No dense material such as a filament is visible at the location of the burst.

A magnetogram image of the entire active region is shown in Figure 4, with the radio positions superposed. The 15 GHz VLA source position, shown by the cross, lies on the magnetic inversion line, about 6″ east of the Hα brightening shown in Figure 3*b*. If the Hα brightening marks the footpoint of the loop emitting in radio, then the whole loop is not visible at 15 GHz. The other end of the loop is presumed to lie in the bright

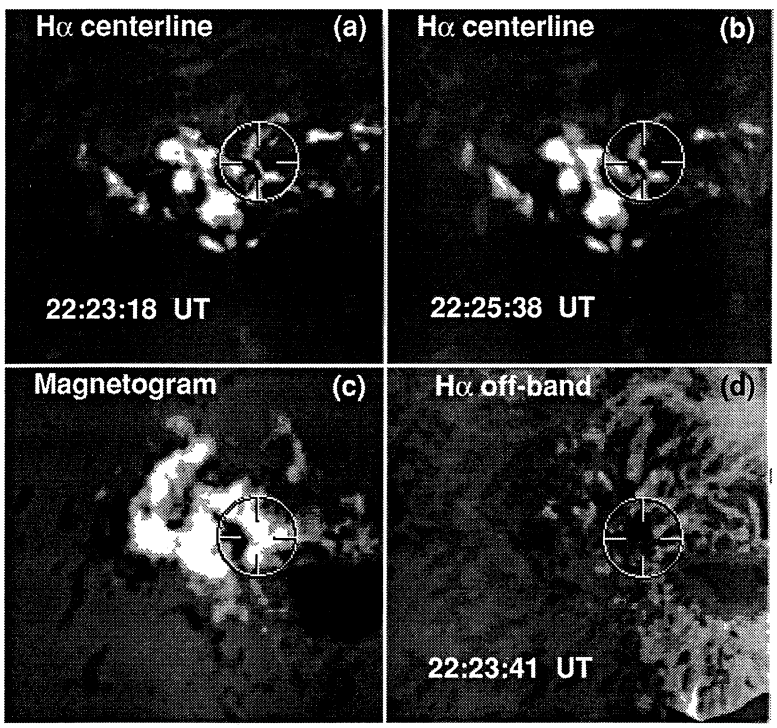

FIG. 3.—Optical data for the radio burst (from Big Bear Solar Observatory). The four panels show (*a*) an Hα centerline image prior to the burst; (*b*) an Hα centerline image during the burst; (*c*) a magnetogram image of the region; and (*d*) an off-band Hα image during the flare. In the magnetogram bright regions indicate magnetic fields pointing upward from the surface of the Sun while dark regions indicate downgoing fields. The "gun-sight" shows the same location in all four panels. The tiny brightening seen in (*b*) is the only significant change from (*a*) to (*b*), and is close to the location of the radio source (see text). Each panel is 250″ east–west. The direction of celestial north is toward the top of these images; solar north is about 6° clockwise from north.

© American Astronomical Society • Provided by the NASA Astrophysics Data System

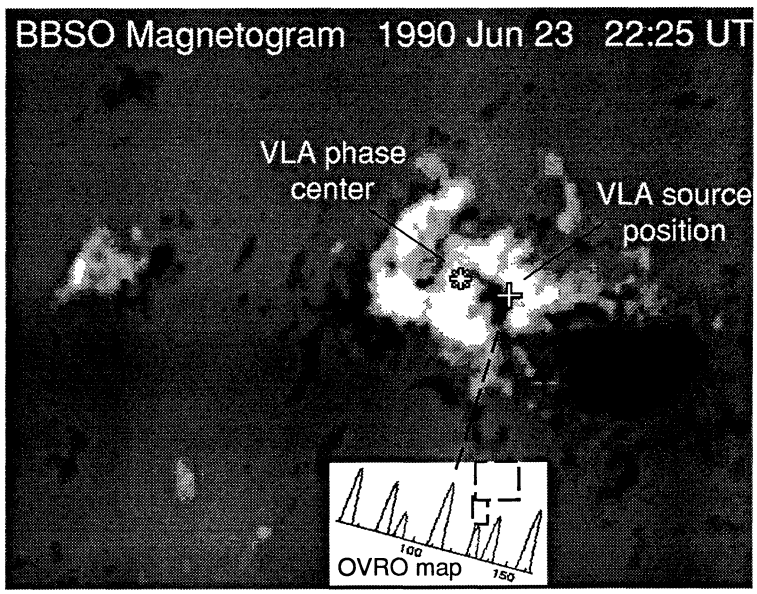

FIG. 4.—A BBSO magnetogram of the active region with the VLA source position and the VLA pointing center given, and the OVRO one-dimensional map superposed. The peaks in the OVRO map correspond to the different fringes of the three-element one-dimensional interferometer pattern, with the most likely location of the burst being at the largest peak (and coincident with the VLA location), but with some chance that it is coincident with one of the other peaks. The image is 400″ east–west and the direction of celestial north is toward the top of the image.

plage to the southeast, where the magnetic polarity has the opposite sense, and any small Hα flash there might not be detectable. The OVRO map at 8.6 GHz, based on only three, colinear baselines, is consistent with the VLA location and with the source dimension measured by the VLA.

3. BURST SOURCE MODELS

The radio spectrum of this event is remarkable (Fig. 5). It is flat or slightly falling from 8.6 to 86 GHz with a flux density near 2 sfu. However, there was no emission at 5 GHz, with a 3 σ upper limit of approximately 0.1 sfu. The time profiles at 8.6, 15, and 86 GHz were apparently identical throughout the burst. A successful interpretation of the burst must account for these features as well as the observed expoential decay rate, a source size constant in time, and a peak brightness temperature of 10^7 K at 15 GHz. At the outset we will state that, despite the excellent information we have for this burst at a broad range of wavelengths, we have been unable to find a plausible model which explains all the details. In this section we sketch out three models which address many of the puzzling features.

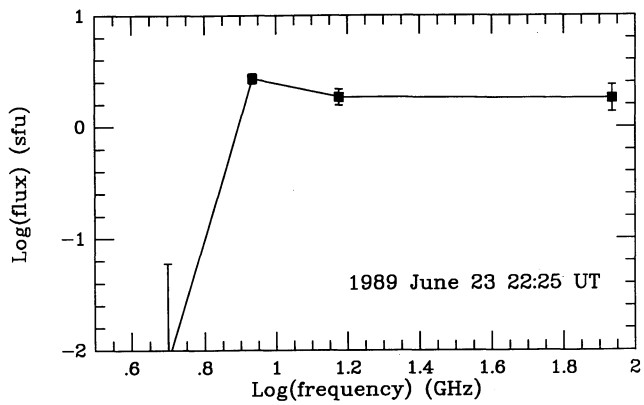

FIG. 5.—The radio spectrum of the burst: the logarithm of the flux (sfu) is plotted against the logarithm of the frequency (GHz). The spectrum is plotted at the time of the peak, 22:25:08 UT, but the spectrum has the same shape at all other times. Error bars at $\pm\sigma$ are shown at 8.6, 15, and 86 GHz, while at 5.0 GHz the upper limit to the flux (~0.06 sfu) is shown.

On the basis of the essentially identical nature of the flux variation with time at 8.6, 15, and 86 GHz, two points can be made. First, the source must either be optically thin for the duration of the event, or it must be optically thick. If a transition from optically thick to optically thin emission were to occur during the burst, or vice versa, then delays between the various frequencies are expected because the transition would occur at different frequencies at different times. Second, the source is probably highly homogeneous, because in an inhomogeneous source radiating via any optically thick mechanism, or via nonthermal gyrosynchrotron emission, different frequencies would arise at different spatial locations, and one then requires uniform evolution across the whole source to explain the observed similarity of the time profiles. An inhomogeneous source of thermal emission would give similar profiles at all optically thin frequencies, but the spectrum is too flat for the thermal gyrosynchrotron mechanism, and thermal bremsstrahlung does not seem to explain the event for reasons discussed below.

The sharp low-frequency cutoff is perhaps the most puzzling aspect of this event. The steep falloff in the spectrum below 8 GHz (spectral index at least 6) cannot be due to the turnover of a self-absorbed bremsstrahlung spectrum. The obvious explanation of such a falloff is a cutoff due to the plasma frequency. A plasma frequency in the range 5–8.6 GHz requires a density of 3.0–9.0 × 10^{11} cm^{-3}. This density may be present in the emission region, or between us and the emission region. We note that the cutoff is steeper than one expects for Razin suppression, unless the plasma frequency is almost 5 GHz (e.g., see Ramaty 1969 and Klein 1987). An alternative explanation is

© American Astronomical Society • Provided by the NASA Astrophysics Data System

that gyroresonance absorption produces the cutoff. This would require a magnetic field of only 600 G along the line of sight, if the absorption is at the third harmonic. This effect has also been seen previously (Dulk, Bastian, & Kane 1986), but in that case the flare was on the limb and the radiation had to pass over a sunspot en route to Earth. The gyroresonance absorption explanation requires that the magnetic field strength increase with height along the line of sight, which is less likely for this burst located at E30 than for a limb event. However, we note that the burst peak lies over a neutral line.

We note that Castelli et al. (1974) also reported microwave bursts with properties similar to those here. With the Sagamore Hill fixed-frequency receivers they observed a number of bursts, all from the same region on 1972 July 31, which showed emission only at high (>9 GHz) frequencies and with sharp cutoffs on the low-frequency side of the spectrum. They noted that these were unusual bursts and attributed the spectrum to exceptionally high magnetic fields in the radio source (~2000 G). However, they were unable to say much about the high-frequency side of the spectrum due to the inadequate sensitivity of their 35 GHz receiver and assumed that the spectra were falling off at high frequency, unlike the burst discussed here. Their bursts had peak fluxes of 20–100 sfu at 15 GHz, and X-ray emission was seen from nearly all bursts. Castelli et al. (1974) interpreted the low-frequency cutoff as gyroresonance absorption along the line of sight.

We now discuss models for the burst spectrum. The observations are consistent with a flat-flux spectrum or a shallow power law (index -0.2). Such a flat spectrum can be compatible with optically thin thermal bremsstrahlung, a collisionally absorbed, optically thick gyrosynchrotron spectrum, or an optically thin gyrosynchrotron spectrum.

3.1. *Optically Thin Thermal Bremsstrahlung Model*

Optically thin thermal bremsstrahlung naturally has a flat spectrum (e.g., see the curves in Dulk 1985; the spectral index is actually about -0.1 when the frequency-dependence of the Gaunt factor is taken into account). The density deduced above based on the assumption that the low-frequency cutoff is a plasma frequency effect is a very high density for a solar flare but is in fact consistent with the observed spectrum if emission is optically thin bremsstrahlung. The peak brightness temperature at 15 GHz determined by the VLA was 10^7 K. Since the source is still optically thin at 8.6 GHz, $T_e > 3 \times 10^7$ K. If we adopt a line-of-sight depth through the source equal to the smallest linear dimension, about 1.5×10^8 cm, then the observed brightness temperatures require $n_e^2 T_e^{-1.5} = 8.2 \times 10^{10}$ cm^{-6} K$^{-1.5}$. With the constraint on T_e, this implies $n_e > 6.7 \times 10^{11}$ cm^{-3}. Thus both the observed cutoff in the spectrum and the observed brightness temperatures independently require a very high density in the source, and this density is very tightly constrained:

$$6.7 \times 10^{11}\left(\frac{L}{1.5 \times 10^8}\right)^{-1} < n_e < 9.2 \times 10^{11} \text{ cm}^{-3} . \quad (1)$$

The upper limit corresponds to a plasma frequency of 8.6 GHz.

Temperature is similarly constrained by the spectrum and the limits on density:

$$3 \times 10^7 \text{ K} < T_e < 1.1 \times 10^8\left(\frac{L}{1.5 \times 10^8 \text{ cm}}\right)^2 \text{ K} . \quad (2)$$

We note that the thermalization time in such a plasma is on the order of 1 millisecond, and we can thus expect it to have a Maxwellian distribution to a high degree of accuracy.

The observation by the VLA of polarization at 15 GHz allows us to determine the magnetic field strength within the source. Thus a degree of polarization of 26% gives $B \cos \theta = 700$ G, according to the standard theory of free-free polarization, where θ is the angle between B and the line of sight. In a 700 G field the magnetic energy density, 2×10^4 ergs cm^{-3}, is still more than adequate to contain the thermal energy density of the flare plasma, 3×10^3 ergs cm^{-3}, and thus we do not expect any expansion of the source.

We note that B is in principle constrained from above by the lack of detection of optically thick gyroresonance emission at 8.6 or 15 GHz. The gyrofrequency is 2.0/cos θ GHz. For cos $\theta = 0.8$, with the above parameters, optically thick cyclotron lines would be seen at 10 and 12.5 GHz. For cos $\theta = 0.6$, optically thick cyclotron lines would occur at 13 and 16 GHz (assuming a magnetic scale height in excess of 2×10^7 cm). In the absence of observations at frequencies between 8.6 and 15 GHz, we cannot be sure that such lines (whose bandwidth would be of order 5%–10%) were not present in the spectrum and thus cannot give an upper limit to B.

The BIMA data show a remarkably linear variation of flux with time in the rise phase at this flare. At this point we come to the first major difficulty in interpreting this flare. Due to the inverse dependence of bremsstrahlung opacity on temperature, it is straightforward to show that any increase in the temperature of the source must lead to a decrease in the observed radio brightness temperature, for optically thin emission with constant density. Consequently we cannot explain the rise by an increase in temperature alone (note that the excellent agreement of the 8.6, 15, and 86 GHz time profiles excludes the possibility of optically thick emission at any stage before the late decay phase). Cooling of plasma even hotter than 3×10^7 K can be ruled out because the initial temperature would have to be extreme and the hotter plasma would emit strongly via the thermal gyrosynchrotron process. This was not seen.

Having ruled out temperature changes alone, we must rely mainly on an increase in density to explain the observed time profile. An isothermal compression would require that density increase with $t^{1/2}$. Physically more plausible is an adiabatic compression (Maetzler et al. 1978). During such a compression $T_e V^{2/3} =$ constant, where V is the source volume, and $\aleph = n_e V$, the total number of particles, is constant. The bremsstrahlung optical depth is $0.2 n_e^2 T_e^{-1.5} f^{-2} L$, where L is the dimension of the source along the line of sight. We find that the dependence of flux $S \propto \Delta\Omega T_b f^2$ on the parameters can be reduced to ($\Delta\Omega \propto$ area A)

$$S \propto \frac{\aleph^2}{V^{2/3}} . \quad (3)$$

Hence the observed increase in flux by a factor of at least 30 (based on the BIMA profile) can be explained by a decrease in volume by 150, with a corresponding increase in temperature of ~30. This would put the initial temperature at 10^6 K, i.e., a typical coronal temperature, and the initial density at 5×10^9 cm^{-3}. The linear rise in brightness flux observed implies that the compression proceeds as $V \propto t^{-3/2}$.

The principal difficulty with this interpretation is that no change in source size is seen by the VLA 15 GHz observations. The BIMA and OVRO observations might not easily detect

© American Astronomical Society • Provided by the NASA Astrophysics Data System

such a change in source size due to the fact that large sources cannot be detected, but the VLA configuration contains sufficient short spacings that they should see such a change during the rise phase (about four integration points). This implies that any compression must occur to numerous small structures within the envelope of the source. However, if the filling factor is small then the true brightness temperature in the source must be larger than assumed, and correspondingly the densities must also be larger. But density and temperature are tightly constrained by (1) and (2). In addition, if many small regions are compressed it seems unlikely that identical conditions will pertain in each of them; we expect that a number may have densities below 3×10^{11} cm^{-3} and contribute at 5 GHz, while others will have densities above 9×10^{11} cm^{-3} and prevent the 8.6 GHz time profile from following the 86 GHz profile so well. Further, during all but the last part of compression the plasma frequency will be below 5 GHz; since $S \propto n_e^{2/3}$, we should expect to see a flux of at least 1 sfu at 5 GHz just before the density exceeds 3×10^{11} cm^{-3}. This was not seen. We also note that the rise and decay are different, which distinguishes this event from those for which adiabatic heating was originally suggested (Maetzler et al. 1978).

The conditions in the burst source closely resemble those deduced for the soft X-ray loops frequently seen in the decay phases of large flares (Cheng & Widing 1975; Kahler, Krieger, & Vaiana 1975). The cooling of these loops has been discussed extensively, and we will follow that discussion (Moore et al. 1980; Antiochos & Krall 1979; Antiochos 1980a, b; Nagai 1980; Doschek et al. 1982) here. We note at the outset three differences between the soft X-ray loops and the flare here: the soft X-ray loops occur in the decay phase; their decay times are generally longer than found here by at least a factor of 4; and the high density deduced here cannot be due to evaporation, as was concluded in the *Skylab* Workshop (Moore et al. 1980), because of the rapid rise time shown here.

There are three main sources of heat loss apart from adiabatic cooling: radiative cooling, conductive cooling, and enthalpy loss (hot particles leaving the source, carrying heat with them). A source may also cool by evaporation of conductively heated chromospheric material which rises into the source (Antiochos & Krall 1979); however, here we exclude any mechanism which would cause density to rise significantly during the decay phase.

The time scales for the three mechanisms are (Antiochos 1980b): (i) radiative cooling,

$$\tau_r \approx \frac{\frac{3}{2}P}{n_e^2 \Lambda(T_e)} \sim 1000 \text{ s} \quad (4)$$

where $P = (n_i + n_e)k_B T$ is the pressure and $\Lambda(T_e)$ the radiative cooling function (e.g., Cox & Tucker 1969); (ii) conductive cooling,

$$\tau_c \approx \frac{\frac{3}{2}Pl\,\Delta L}{10^{-6}T_e^{7/2}} \sim 24\,\frac{\Delta L}{10^8 \text{ cm}} \text{ s}\,, \quad (5)$$

where l is the loop length (4×10^8 cm) and ΔL is the distance over which we calculate the temperature gradient; and (iii) enthalpy losses, for which the time scale is related to the propagation time of sound along the flux tube,

$$\tau_e \approx \frac{l}{c_s} \sim 5 \text{ s}\,, \quad (6)$$

where $c_s = 8 \times 10^7$ cm s^{-1}.

These numbers imply that radiative cooling is too slow to be relevant to this problem until the source has cooled greatly, while conductive cooling has the correct time scale. The sound propagation time is shorter than the observed decay time scale, indicating that pressure equilibrium is likely to apply along the flux tube during the decay, and that mass motions will occur at the ends of the flux tube containing the source if a pressure imbalance exists there (Craig & McClymont 1976). Chromospheric material will be heated until its pressure is sufficient to prevent further mass motion from the corona.

Before proceeding, we note two difficulties. If the source simply cools by heat conduction with no change in density, the observed brightness temperature should actually increase. On the other hand, if the density decreases isothermally, which will decrease the observed T_b, then the 5 GHz flux will become detectable when the plasma frequency drops below 5 GHz. In the worst case the plasma frequency will drop from 8.4 GHz to 4.8 GHz before the 5 GHz emission becomes visible; at that point the flux in an isothermal decay should be 0.16 sfu at all frequencies (about 60 s after the peak). Such a flux level would have been easily detected at OVRO. We can avoid this difficulty if the temperature rises while the density drops: thus, if T_e increases by a factor of 10 before the plasma frequency drops below 5 GHz, the predicted flux would be only 0.05 sfu.

As described in the papers referred to above, soft X-ray loops should cool as follows. Initially conduction dominates. The energy passes into the chromosphere and transition region, where it is radiated away more efficiently by the cooler plasma. As the temperature and density in the source decrease, the coronal plasma begins to collapse downward, while there is also motion of heated chromospheric material upward. However, the simulations do not show exponential decays in any parameter. Indeed, to model one case in which the observed decay shows a long tail Antiochos & Krall (1979) were forced to use four loops, each of which peaked at different times, in order to fit the decay curve. In general, decay was much faster than exponential. One important difference in this case is that the sound propagation time is shorter than the conductive cooling time, unlike previous simulations.

No soft X-ray emission was seen in the *GOES* records at the time of the radio burst, and this also presents a difficulty for the thermal free-free model. If we assume a density of 7×10^{11} cm^{-3}, a temperature of 3×10^7 K and a volume of 3×10^{24} cm^3, then the resulting emission measure should produce a flux of at least 3×10^{-6} W m^{-2} in the 1–8 Å band (Thomas, Starr, & Crannell 1985). However, inspection of the *GOES* data indicates that the 1–8 Å flux due to the burst did not exceed 3×10^{-7} W m^{-2}.

Finally in this discussion we must return to examine emission in the vicinity of the plasma cutoff. Until now we have ignored the effect of the cutoffs on the bremsstrahlung emissivity. However, by analogy with the Razin-Tsytovich effect (Razin 1957), we expect that there will be some effect. Melrose (1972) has discussed the relativistic bremsstrahlung analogy of the Razin-Tsytovich effect, and Zheleznyakov (1970) shows the bremsstrahlung emissivity as being proportional to refractive index, but we can find no discussion in the literature which clearly applies to the situation here. We have carried out an analysis (to be presented elsewhere) and find that the emissivity is proportional to the refractive index as well as other factors depending on mode properties. We find that the cutoff due to the plasma frequency is probably not sharp as assumed, and this presents another difficulty for the optically thin thermal

© American Astronomical Society • Provided by the NASA Astrophysics Data System

bremsstrahlung model. We also note that the two modes (x and o) have cutoffs separated by about half the gyrofrequency, and this argues that the plasma frequency is closer to 5 than to 8.6 GHz.

3.2. *Gyrosynchrotron Emissivity with Bremsstrahlung Opacity (Optically Thick)*

A free-free absorbed gyrosynchrotron spectrum has previously been proposed (Ramaty & Petrosian 1972) to explain flat-spectrum observations of solar flare radio emission (Hachenberg & Wallis 1961). The idea is that the emission is optically thick due to collisional thermal damping but that the emissivity is characterized by the nonthermal gyrosynchrotron mechanism while the absorptivity is provided by the thermal plasma. This will be the case as long as the gyrosynchrotron emissivity exceeds the bremsstrahlung emissivity and the collisional opacity exceeds the gyrosynchrotron opacity. Ignoring angular dependences for illustrative purposes, we can express the nonthermal gyrosynchrotron emissivity as

$$\eta(f) \propto NB^{0.90\delta - 0.22} f^{1.22 - 0.90\delta}, \quad (7)$$

where N is the number of fast electrons in a power-law tail above some threshold energy, and δ is the spectral index of the nonthermal electron energy distribution. With the absorption coefficient that due to collisional damping,

$$\kappa(f) \propto f^{-2} T_e^{-1.5} n_e^2, \quad (8)$$

the source function is

$$\sigma(f) = \frac{\eta(f)}{\kappa(f)} \propto N n_e^{-2} T_e^{1.5} B^{0.9\delta - 0.22} f^{3.22 - 0.9\delta}. \quad (9)$$

Note that a flat spectrum is obtained for the relatively unremarkable value $\delta = 3.58$. We will refer to models which assume a source function of this type as "GS/thermal" models. A high ambient density is required in this model in order to provide enough thermal opacity, and it simultaneously explains the low-frequency cutoff.

Such models avoid some of the problems found in the optically thin bremsstrahlung model. The simultaneity of the maximum at each frequency is easily explained, since it presents a problem only to those models which rely on a transition from optically thick to optically thin emission, or vice versa. Here we assume optically thick emission throughout and the flux simply tracks the brightness temperature (which equals the effective temperature, which embodies the source function, which is frequency-independent). The evolution of the source size, which was a serious problem for the compression model discussed above in that the 15 GHz source size does not seem to change significantly in time, is easily explained by the GS/thermal model. The collision frequency of a fast particle in a colder plasma is given by $f_{\rm coll} = 1.38 \times 10^{-9} n_e Z^2 \ln(\Lambda) E_{\rm keV}^{-1.5}$ s^{-1}, where $\ln(\Lambda)$ is the Gaunt factor. For a 100 keV electron in a solar plasma, the collision frequency is about 20 s^{-1} and the mean free path is about 5×10^8 cm. This is about the loop length, and so, once accelerated, electrons with energies above 100 keV quickly distribute themselves throughout the loop volume. While the collisional scattering time is sufficiently long that the fast electrons are easily distributed throughout the loop volume, the scattering time is much shorter than either the rise or decay times, and thus the fast electron numbers would decrease on this time scale without replacement. On this basis it would appear that continuous acceleration is required throughout the event, and therefore that the time profile of the event represents the envelope of the energy release profile (or at least of the resulting acceleration of fast electrons).

However, there are other severe problems with the GS/thermal model here. In order to keep the source optically thick at 86 GHz, with the density of the cool plasma specified by the plasma cutoff (we use 5×10^{11} cm^{-3}) and the line-of-sight depth (1.5×10^8 cm) known, the temperature must be below 10^6 K. Since we know the energy spectrum of the nonthermal electrons, we can now place a constraint on the magnetic field and on the density of the fast particles by requiring that the ratio of the gyrosynchrotron emissivity to the collisional opacity gives a source function with a temperature of 10^7 K at 15 GHz. One requires that the following product be satisfied:

$$(\sin\theta)^{1.86}\left(\frac{B}{100\ \rm G}\right)^3\left(\frac{N}{10^6\ \rm cm^{-3}}\right)\left(\frac{T_e}{10^6\ \rm K}\right)^{1.5} = 1 \times 10^5. \quad (10)$$

In deriving densities from this formula we will use $\theta = 45°$.

Another consideration argues that the temperature in the thermal plasma cannot be as high as 10^6 K. The thermal emissivity is flat in frequency, whereas the gyrosynchrotron emissivity falls off with frequency squared. Thus above some frequency the thermal emissivity must dominate, and the flux spectrum must revert to pure optically thick thermal emission ($S \propto f^2$). As might be expected, this will occur when the apparent brightness temperature drops from above to below the temperature in the thermal source. Since the implied brightness temperature at 86 GHz is 3×10^5 K, the temperature in the dense plasma cannot exceed this. With this temperature and with $B = 500$ G, a nonthermal density of 2×10^9 cm^{-3} is needed. But since the radiative cooling time of plasma with a density of 5×10^{11} cm^{-3} at 3×10^5 K is about 0.1 s, either this plasma is being replenished continually or else it must actually be much cooler. A more reasonable temperature is then 2×10^4 K, for which equation (10) requires a nonthermal density (above 10 keV) of 3×10^{11} cm^{-3} if the magnetic field is 500 G. The resulting energy density of nonthermal electrons exceeds the magnetic field energy density. In fact most of the radio emission will come from the electrons with higher energies; we require a nonthermal density of only 7.9×10^8 cm^{-3} if there is a low-energy cutoff in the nonthermal distribution at 100 keV. The energy density of the nonthermal particles is then less than the magnetic field energy: 2×10^2 ergs cm^{-3}, compared with 10^4 ergs cm^{-3} in the background magnetic field, and 1 ergs cm^{-3} in the thermal plasma.

Conversely, we must also ensure that at the low-frequency end the gyrosynchrotron opacity does not exceed the thermal opacity, which would result in the usual self-absorbed gyrosynchrotron spectrum. This leads to the following condition at 8 GHz:

$$(\sin\theta)^{2.49}\left(\frac{B}{100\ \rm G}\right)^{3.81}\left(\frac{N}{10^6\ \rm cm^{-3}}\right)\left(\frac{T_e}{10^6\ \rm K}\right)^{1.5} < 3 \times 10^6. \quad (11)$$

This is in fact easily satisfied if equation (10) is satisfied.

We can use the expected degree of polarization of gyrosynchrotron and bremsstrahlung emission to obtain a formula for the polarization of the GS/thermal model, and then find values of B and θ which give 26% polarization at 15 GHz. We find that at $\theta = 5°$ we need $B = 5$ G; at $\theta = 25°$ we need $B = 15$ G; at $\theta = 45°$ we need $B = 80$ G; at $\theta = 65°$ we need $B = 270$ G; and at $\theta = 85°$ we need $B = 460$ G. These

© American Astronomical Society • Provided by the NASA Astrophysics Data System

values should be regarded as rough estimates only, but they indicate that the polarization can easily be accounted for in this model with plausible parameters.

However, the energy input into the plasma by the collisional cooling of the fast electrons will rapidly heat up the ambient plasma because it cannot radiate the energy away fast enough at chromospheric temperatures. In the temperature range between 2×10^4 K and 10×10^4 K the cooling rate goes roughly as T_e^2 (Cox & Tucker 1969), and this must be proportional to the number of fast electrons injected. Hence the source function which determines the time evolution of the flux we see varies as

$$\sigma(f) \propto \frac{N}{T_e^{-1.5}} \propto N^{7/4} .$$

When one takes this temperature change into account, the energetics depend on the low-energy cutoff in the energy spectrum of the nonthermal electrons. Combining equation (10) with the equation balancing the heat input to the thermal plasma from the nonthermal electrons and the radiative losses (conduction losses are unimportant at low temperatures), one finds that unless the cutoff is at least 0.5 MeV the peak temperature is well above the peak in the cooling curve at about 2×10^5 K, and thermal runaway will take place, the plasma being unable to radiate away the energy input from collisions no matter what the temperature. This would then make the plasma optically thin at 86 GHz, violating an assumption of the model. Another difficulty with the model is that for the parameters in the GS/thermal model the Razin frequency would be well above the observing frequencies unless the magnetic field in the source is high ($\sim$1000 G); however, such a high field would put the 8.6 GHz emission at the third gyroharmonic, and the gyrosynchrotron parameters do not then apply.

Thus the GS/thermal model can explain the observations only if the density of nonthermal particles is very high, and their energy density dominates the plasma. This is difficult to understand, since the nonthermal particles must be continuously regenerated without any obvious source of energy large enough to produce them.

3.3. *Optically Thin Gyrosynchrotron Emission in a Homogeneous Source*

Here we assume a very hard spectrum of electrons to produce a flat spectrum. The emission must be optically thin from 8.6 to 86 GHz to explain the similarity of the time profiles across that frequency range. The low-frequency cutoff must be due to free-free or gyroresonance absorption by intervening material, since the Razin-Tsytovich effect is not sharp enough to explain the observed spectrum.

Let us adopt a spectral index of $\delta = 1.4$; then we can use the Dulk & Marsh (1982) formulae (Dulk 1985) to estimate other source parameters assuming a homogeneous magnetic field and density. We find that if $\cos\theta = 0.10$, then $B = 540$ G and $N = 7 \times 10^3$ cm^{-3}; if $\cos\theta = 0.707$, then $B = 100$ G and $N = 5 \times 10^4$ cm^{-3}; and if $\cos\theta = 0.90$, then $B = 30$ G and $N = 3 \times 10^5$ cm^{-3}. These values are quite reasonable, and indeed resemble the parameters for another flare which also seemed to be optically thin gyrosynchrotron emission with a flat spectrum (Kundu, Velusamy, & White 1987). In that case an inhomogeneous source model with a steeper electron energy spectrum deduced from hard X-ray observations could also fit the flat radio spectrum up to 15 GHz (Nitta et al. 1991); such a model cannot work here because it cannot be extended to 86 GHz (it would require implausibly high magnetic fields).

Thus the main drawback of this model is that we need either high-density material or high magnetic fields in the corona along the line of sight between us and the gyrosynchrotron source. Since the active region was at about N30E30 at the time of the flare, we require material higher in the corona than the source to provide the absorption, and it must cover the whole source. There was no evidence for dense material such as filament material over the radio source location in the Hα images.

4. CONCLUSION

We have presented radio observations of a simple impulsive solar burst covering over a decade in frequency, from three observatories providing complementary information. The striking observational aspects of this flare are that the time profile was identical throughout at 8.6, 1.5, and 86 GHz, that the spectrum was flat from 8.6 to 86 GHz, and that there was a sharp cutoff in the spectrum between 5.0 and 8.6 GHz. The similarity of the time profiles at all frequencies down to low flux levels implies that the same emission mechanism must be operating from 8.6 to 86 GHz. The simplest interpretation of the cutoff, namely as a plasma frequency effect, leads to the conclusion that there was exceptionally high density in the solar corona ($\sim 5 \times 10^{11}$ cm^{-3}). Such high densities have been seen in solar flares previously (e.g., Neupert 1971; Marsh & Hurford 1980; Feldman, Doschek, & Kreplin 1982; Hoyng et al. 1983), but usually in the decay phase of the flare when high-density, soft X-ray–emitting flare loops are also seen. In those cases the high density has been attributed to chromospheric evaporation (Moore et al. 1980). Here the high density must be present at the onset of the flare. This seems unusual given the impulsive time scale of this event. It is possible that the high density is not present in the emitting source itself, but rather is foreground material along the line of sight.

We explored three models for this flare. The model in which the emission is optically thin thermal bremsstrahlung naturally explains the flat spectrum and the sharp cutoff, but the time evolution must reflect the evolution of the electron density in the source, and it is difficult to envisage physical processes which can reproduce what is seen; further, the parameters for such a source imply an order of magnitude more soft X-ray emission than was seen by the *GOES* detectors. The optically thick GS/thermal model, in which emissivity is provided by nonthermal gyrosynchrotron emission and opacity by collisional absorption, can also explain the same features and implies that the time evolution reflects the acceleration of the nonthermal particles. However, the required number density of the nonthermal electrons is high and their energy density must dominate the plasma unless there is a low-energy cutoff to the distribution above about 50 keV. Optically thin gyrosynchrotron emission by a very hard spectrum of electrons which is absorbed by dense material along the line of sight can also explain the event, but such a hard spectrum presents a problem for acceleration mechanisms and such high-density material covering a large area is not normally seen in the corona. Other models, such as that the material is initially present as very dense but neutral gas which is suddenly heated and ionized, may be relevant. However, mechanisms for impulsively heating neutral material in the solar corona have not been explored in much detail.

© American Astronomical Society • Provided by the NASA Astrophysics Data System

This burst is clearly not characteristic of most solar microwave bursts; further observations are required to determine whether such bursts are common and how they are related to more typical flares. They can be identified only by sensitive millimeter-wavelength observations in conjunction with microwave observations as was the case here.

We are grateful to A. Kiplinger and the organizers of the first Max '91 campaign for their coordination, and to NASA, NSF, and NOAA for their support of this campaign. We thank the referee for his insightful comments, and particularly for bringing the Castelli et al. (1974) reference to our attention and for pointing out the incompatibility of the *GOES* observations with the thermal free-free model. Research at University of Maryland was supported by NSF grant ATM 87-17157 and NASA grants NAG-W-1541 and NAG-W-2172; research at University of California-Berkeley was supported by NSF grant AST 87-14721; research at University of Colorado was supported by NASA grants NSG-7287, NAGW-1994, and NAG5-1322; and research at Caltech was supported by NSF grants ATM 90-13173 and AST 89-19770.

REFERENCES

Antiochos, S. K. 1980a, ApJ, 236, 270
———. 1980b, ApJ, 241, 385
Antiochos, S. K., & Krall, K. R. 1979, ApJ, 229, 788
Castelli, J. P., Guidice, D. A., Forrest, D. J., & Babcock, R. R. 1974, J. Geophys. Res., 79, 889
Cheng, C.-C., & Widing, K. G. 1975, ApJ, 201, 735
Cox, D. P., & Tucker, W. H. 1969, ApJ, 157, 1157
Craig, I. J. D., & McClymont, A. N. 1976, Sol. Phys., 50, 133
Doschek, G. A., Boris, J. P., Cheng, C.-C., Mariska, J. T., & Oran, E. S. 1982, ApJ, 258, 373
Dulk, G. A. 1985, ARA&A, 23, 169
Dulk, G. A., Bastian, T. S., & Kane, S. R. 1986, ApJ, 300, 438
Dulk, G. A., & Marsh, K. A. 1982, ApJ, 259, 350
Feldman, U., Doschek, G. A., & Kreplin, R. W. 1982, ApJ, 260, 885
Guidice, D. A., & Castelli, J. P. 1975, Sol. Phys., 44, 155
Hachenberg, O., & Wallis, G. 1961, Z. Astrophys., 52, 42
Hoyng, P., Marsh, K. A., Zirin, H., & Dennis, B. R. 1983, ApJ, 268, 865
Hurford, G. J., Read, R. B., & Zirin, H. 1984, Sol. Phys., 94, 413
Kahler, S. W., Krieger, A. S., & Vaiana, G. S. 1975, ApJ, 199, L57
Klein, K.-L. 1987, A&A, 183, 341
Kundu, M. R., Velusamy, T., & White, S. M. 1987, ApJ, 321, 593
Kundu, M. R., White, S. M., Gopalswamy, N., Bieging, J. H., & Hurford, G. J. 1990, ApJ, 358, L69
Maetzler, C., Bai, T., Crannell, C. J., & Frost, K. J. 1978, ApJ, 223, 1058
Marsh, K. A., & Hurford, G. J. 1980, ApJ, 240, L111
Melrose, D. B. 1972, Ap&SS, 18, 267
Moore, R., et al. 1980, in Solar Flares (Skylab Solar Workshop II), ed. P. A. Sturrock (Boulder: Colorado Associated Univ. Press), 341
Nagai, F. 1980, Sol. Phys. 68, 351
Neupert, W. M. 1971, Sol. Phys., 18, 474
Nitta, N., White, S. M., Schmahl, E. J., & Kundu, M. R. 1991, Sol. Phys., 132, 125
Ramaty, R. 1969, ApJ, 158, 753
Ramaty, R., & Petrosian, V. 1972, ApJ, 178, 241
Razin, V. A. 1957, Dissertation (Gorkii: Gorkii State Univ.)
Thomas, R. J., Starr, R., & Crannell, C.-J. 1985, Sol. Phys., 95, 323
Zheleznyakov, V. V. 1970, Radio Emission of the Sun and the Planets (Oxford: Pergamon)

© American Astronomical Society • Provided by the NASA Astrophysics Data System